Positron Annihilation in Metals

S. KAHANA*
Institute for Theoretical Physics, University of Copenhagen, Denmark
(Received 17 September 1962)

An adequate description of positron annihilation rates in metals is obtained by extension of the high-density limit, for annihilation in an electron gas, to realistic densities. A short-range electron-positron force is obtained in the high-density limit and is used to treat accurately the two-body correlations between the positron and metallic valence electrons. This description proves to be satisfactory for metals with low valence electron densities as well. The variation of annihilation rates with valence electron density, and also the absolute rates, agree quite well with those obtained experimentally by Bell and Jørgensen.

I. INTRODUCTION

IN an earlier paper[1] the author discussed the annihilation of positrons in metals using a screened potential based on the Bohm-Pines model for an electron gas.[2] He found a variation in annihilation rates with electron density not indicated by the then current experiments. Subsequently, Bell and Jørgensen[3] remeasured some of the relevant rates and found a variation more or less parallel to that predicted in K(I). However, the annihilation rates of Bell and Jørgensen were considerably less than those obtained by this author.

The present work redoes the calculations of K(I) using a second quantized description of the electron gas, and an approximation scheme guided by the high-density limit for the gas. The principal weakness of the Bohm-Pines approach relevant to our problem is the arbitrariness of the choice of a screening length in the short-range electron-positron force. In the high-density limit one is led naturally to a screened Coulomb force. In this limit one is able to account simply for the polarization of the background medium by an interacting electron-positron pair and to compute the effects of this polarization on annihilation rates. Unfortunately when one approximates real metals by electron gases the electron densities are not in the high-density region. If then we wish to obtain meaningful quantitative results we must look for some way of extending the high-density calculations to regions of lower density.

In K(I) and in the present work we have tried to obtain a description valid for realistic densities by accurately accounting for the two-body correlations between the positron and an annihilating electron. The attractive nature of the electron-positron force suggests that these correlations are of greatest importance. They produce a coherent contribution to the electron density in the immediate neighborhood of the positron. No higher order correlations are considered with the exception of those responsible for the screening of the attractive electron-positron force.

In what follows we have first outlined our approach in the high-density limit and then have applied this approach to electron gases which can be used to describe real metals.

II. FORMAL THEORY OF THE ANNIHILATION AND THE EFFECTIVE ELECTRON-POSITRON FORCE

A calculation of the annihilation rate reduces essentially to estimating the electron density at the positron averaged over all positron positions.[4] This quantity is

$$n=\int\langle(\psi_{(x)}{}^{\dagger}\psi_{(x)})(\phi_{(x)}{}^{\dagger}\phi_{(x)})\rangle d^3x. \tag{1}$$

We are using a second quantized notation in which $\phi(x)$ is the positron Heisenberg field at time t and position x; while $\psi(x)$ is the corresponding electron field.[5] The expectation value in (1) is taken in the fully interacting ground state for the system of electrons and positron. It is possible to relate (1) to the zero-temperature electron-positron correlation or Green's function. The latter is defined as

$$G_{ep}(xy;x'y')=i^2\langle|T(\psi(x)\phi(y)\phi^{\dagger}(y')\psi^{\dagger}(x'))|\rangle, \tag{2}$$

where T is the Wick time-ordering operator.[6] We see then

$$n=(-i)^2\int d^3x\lim_{t'\to t+}G_{ep}(xt,xt;xt',xt'). \tag{3}$$

If the positron were uncorrelated with its neighboring electrons we would have as an approximation to (2)

$$G_{ep}(xy;x'y')=G_e(x,x')G_p(y,y'), \tag{4a}$$

* This work was performed while the author was on leave of absence from the Mathematics Department, McGill University, Montreal, Canada. The author would like to express his gratitude to the Ford Foundation for support during his stay in Copenhagen and to the National Research Council of Canada for aid in travelling.

[1] S. Kahana, Phys. Rev. **117**, 123 (1960). Referred to in future as K(I).

[2] D. Bohm and D. Pines, Phys. Rev. **92**, 609 (1953).

[3] R. E. Bell and M. H. Jørgensen, Can. J. Phys. **38**, 652 (1960).

[4] R. A. Ferrell, Rev. Mod. Phys. **28**, 308 (1956).

[5] We are suppressing the spin labels on the field operators. One must of course remember that the annihilation into two quanta can only take place from the singlet spin state and we incorporate this into later calculations of the annihilation rates. Once the density is calculated we can calculate the annihilation rate R by comparison with the known density and rate in positronium. The result is

$$R=\tfrac{1}{4}R_{\text{positronium}}(n/n_{\text{positronium}}).$$

The factor $\frac{1}{4}$ arises from a spin averaging which is clearly required in a metal.

[6] G. Wick, Phys. Rev. **80**, 268 (1950).

where

$$G_e(x,x')=i\langle T(\psi(x)\psi^\dagger(x'))\rangle \tag{4b}$$

and

$$G_p(x,x')=i\langle T(\phi(x)\phi^\dagger(x'))\rangle. \tag{4c}$$

It is to be noted that the single-particle Green's functions in (4) are expectation values of Heisenberg operators in the fully interacting ground state. Nevertheless translational invariance assures us that the density, n, obtained by use of (4) as a first approximation to (2) does not differ from that for a positron inserted into a sea of electrons with which it does not interact. Thus inclusion of only self-energy effects within the electron gas cannot alter the annihilation rate from its free or Sommerfeld value. In the following analysis we ignore all self-energy effects, including the interaction of the electron and positron with the metallic lattice, even though these are ultimately of great interest.

The equations of motion for the fully interacting system couple the particular Green's function (2) to functions involving both fewer and greater numbers of particle coordinates.[7] It will be possible, however, to restrict our attention to a single integral equation for G_{ep}. Formally we may write

$$G_{ep}(xy,x'y') = G_e^0(xx')G_p^0(yy')+(-i)\int d\xi d\eta d\xi' d\eta' \times G_e^0(x\xi)G_p^0(y\eta)I(\xi\eta;\,\xi'\eta')G_{ep}(\xi'\eta',x'y'). \tag{5}$$

G_e^0 and G_p^0 are Green's functions for freely propagating electron and positron. I is an interaction operator which is formally defined by (5) but which may be computed from a perturbation expansion for G_{ep}.

If a definite choice is made for the interaction operator then (5) may provide a means for producing quantitative results. The simplest choice that suggests itself is to set

$$I=v_{ep},$$

i.e.,

$$(xy|I|x'y')=v_{ep}(x-y)\delta^4(x-x')\delta^4(y-y'), \tag{6a}$$

where

$$v_{ep}(x-y)=(e^2/|\mathbf{x}-\mathbf{y}|)\delta(t). \tag{6b}$$

The time δ function in (6b) reminds us of the instantaneous or static nature of the Coulomb force. On physical grounds it is clear that (6a) is inadequate. The positron in addition to interacting directly with an electron will appreciably polarize the surrounding gas. The resulting polarization charge will then screen and weaken the direct interaction between electron and positron.

For a very dense electron gas one would expect to be able to expand G_{ep} in powers of the electron-positron or electron-electron Coulomb potentials, and retain only the lowest orders. It is, however, necessary to ensure that the polarization is adequately, treated. Following the suggestions of previous authors[8–10] we can partially account for the electron gas polarizability by summing a specific set of terms in perturbation theory; the terms in which the positron before interacting with a given electron, excites a number of particle-hole pairs in the background gas. The series arising in this fashion is represented graphically in Fig. 1.

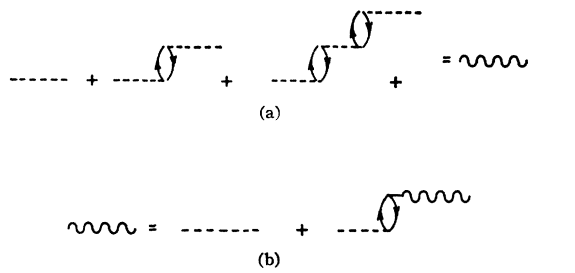

FIG. 1. (a) Diagrammatic representation of the effective electron-positron interaction $u(x)$. (b) Graphical representation of an integral equation for $u(x)$.

The final result is to replace $v_{ep}(x)$ by an effective interaction $u(x)$ indicated schematically by a wavy line in Fig. 1(a). $u(x)$ satisfies the following integral equation [Fig. 1(b)],

$$u(x-y)=v_{ep}(x-y)+(-i)\int dz dz' \times v_{ee}(x-z)G_e^0(z,z')G^0(z,z')u(z'-y), \tag{7}$$

where $v_{ep}=-v_{ep}$ is the electron-electron Coulomb potential. Because of the finite inertia of the background gas the effective interaction is clearly not static.

Equation (7) is readily solved by introducing the Fourier representations,[9,10]

$$u(x)=(1/2\pi V)\sum_k \int d\omega\, e^{i\mathbf{k}\cdot\mathbf{x}-i\omega t}u_k(\omega), \tag{8a}$$

$$v_{ee}(x)=(1/2\pi V)\sum_k \int d\omega\, e^{ikt-i\omega t}v_k, \quad v_k=\frac{4\pi e^2}{k^2}, \tag{8b}$$

$$G_e^0(x,0)=(1/2\pi V)\Big[\sum_{k>k_F}\int d\omega \frac{e^{i\mathbf{k}\cdot\mathbf{x}-i\omega t}}{-\omega+k^2+i\eta} + \sum_{k<k_F}\int d\omega \frac{e^{i\mathbf{k}\cdot\mathbf{x}-i\omega t}}{-\omega+k^2-i\eta}\Big],$$

where V is the quantization volume and k_F is the Fermi

[7] See for example: P. Martin and J. Schwinger, Phys. Rev. **115**, 1342 (1959), or A. Klein and R. E. Prange, Phys. Rev. **112**, 1008 (1958).

[8] M. Gell-Man and K. Brueckner, Phys. Rev. **106**, 369 (1958).
[9] J. Hubbard, Proc. Roy. Soc. (London) **A240**, 539 (1957).
[10] D. F. Dubois, Ann. Phys. (N. Y.) **1**, 174 (1959).

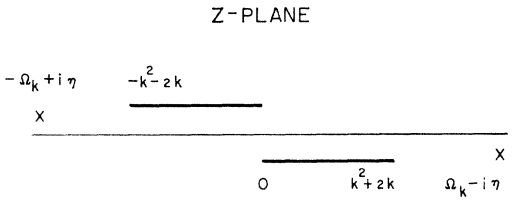

FIG. 2. The z plane indicating the singularities in $u_k(z)$, the Fourier transform of $u(x)$.

momentum of the electron gas. We obtain

$$u_k(\omega)=[1/\epsilon_k(\omega)]v_k, \tag{9a}$$

$$\epsilon_k(\omega)=1+2v_kQ_k(\omega), \tag{9b}$$

$$Q_k(\omega)=\frac{1}{2\pi Vi}\sum_q\int dE\, G_{q+k}(\omega+\epsilon)G_q(\epsilon). \tag{9c}$$

It is natural to regard $\epsilon_k(\omega)$ as a longitudinal dielectric constant for the electron gas. We note this quantity is frequency dependent, reflecting the time dependence of the effective or screened interaction.

Inspection of (9b) and (9c) indicates that $\epsilon_k(Z)$ regarded as a function of the complex variable Z is analytic in the cut plane drawn in Fig. 2. The cuts extend from $Z=-(k^2+2k)$ to $Z=0$ just above the real axis and from $Z=0$ to $Z=k^2+2k$ just below the real axis. These cuts arise from the continuum of possible energies for real electron particle-hole pairs in the non-interacting Fermi sea. The dielectric constant has in addition, zeros at $\omega=\pm\Omega_k$, for values of the momentum transfer k less than some maximum value k_c. It is well known[9,10] that the corresponding singularities in $u_k(\omega)$ are associated with a collective mode of excitation of the electron gas, the plasmon. For $k>k_c$ the plasmon poles merge with the cuts and the plasmon loses its identity as a separate excitation.

Thus the electron-positron interaction is modified by the possible excitation of real electron hole-particle pairs or by the "exchange" of a plasmon between electron and positron. The pair modification produces a short-range or screened force while the plasmon exchange represents residual long-range effects.

In K(I) we identified the plasmon cutoff k_c with a lower limit for the momentum transfer between interacting electron-positron pairs. In effect we took as a screened interaction

$$\begin{aligned} u_k(\omega)&=v_k, \quad k\gtrless k_c \\ &=0, \quad k<k_c. \end{aligned} \tag{10}$$

This arbitrary assignation of a screening length $\sim 1/k_c$ is what we are at present questioning.

Having specified our choice of the interaction I in Eq. (5), i.e.,

$$I(xy;x'y')=u(x-y)\delta^4(x-x')\delta^4(y-y'),$$

we are left with the task of solving the resulting integral equation. This is discussed in the ensuing sections.

III. THE HIGH-DENSITY LIMIT

This limit is obtained by retaining in (5) only the first iterate in the potential $u(x)$. The electron-positron Green's function then becomes

$$G_{ep}=G_e^0G_p^0+G_e^0G_p^0uG_e^0G_p^0. \tag{11}$$

Inserting (11) into (3) yields the high-density annihilation rate. A modification of the Sommerfeld rate is obtained from the first-order term

$$n^{(1)}=\int d^3x\, G_e(xy)G_p(xz)u(y-z) \times G_e(yx)G_p(zx)d^3zd^3y. \tag{12}$$

Fourier transformation yields

$$n^{(1)}=\frac{2i^2}{(2\pi)^2V}\frac{1}{2\pi V}\sum_{\substack{rs,r's'\\ r+s=r'+s'}}\int d\omega d\epsilon dE \times G_r^e(\epsilon+\omega)G_s^p(E-\omega)u_{r-r'}(\omega)G_{r'}^e(\epsilon)G_{s'}^p(E). \tag{13}$$

We must include a specification of the transform of the positron Green's function. We set

$$\begin{aligned} G_k^p(\omega)&=1/(-\omega+k^2-i\eta), \quad k^2>0 \\ &=1/(-\omega+i\eta), \quad k^2=0, \end{aligned} \tag{15}$$

thus imposing the boundary condition that a single positron of zero momentum is originally present in the electron gas.[11]

The integration over the variable E may be performed giving rise to two identical contributions for $s=0$, $s'\neq 0$ and $s\neq 0$, $s'=0$. We obtain

$$n^{(1)}=\frac{2i^3}{(2\pi)^3V^2}\sum_{rs,r's'}\int d\omega\, u_{r-r'}(\omega)2\pi iG_{r'-r}^p(-\omega) \times\left[\int d\epsilon\, G_r^e(\epsilon+\omega)G_{r'}^p(\epsilon)\right]. \tag{16}$$

Reference to (9) allows us to reduce the above to

$$n^{(1)}=\frac{4i}{2\pi V}\sum_{q\neq 0}\int d\omega\, u_q(\omega)Q_q(a)G_{-q}^+(-\omega), \tag{17}$$

where

$$G_{-q}^+(-\omega)=1/(-\omega+q^2-i\eta).$$

The final integration over ω may be completed in the lower half-plane, contributions arising along the positive cut in Fig. 2 and at the associated plasmon pole. The

[11] We are using units in which $2m=\hbar=1$.

result may be written

$$n^{(1)}=n^{(1)}{}_{\text{continuum}}+n^{(1)}{}_{\text{plasmon}}$$
$$=(2/V^2)\sum_{q,p} v_q{}^{\text{h.d.}}[(p+q)^2-p^2+q^2]^{-1}$$
$$+(2/V)\sum_{k<k_c} R_k[k^2+\Omega_k]^{-1} \quad (18)$$

with

$$v_q{}^{\text{h.d.}}=\{|1+2v_qQ_q[(p+q)^2-q^2]|^2\}^{-1}v_q$$

and R_k the residue of $Q_k(\omega)U_k(\omega)$ at Ω_k. There is a clear separation into a potential contribution through the high-density screened interaction $v_q{}^{\text{h.d.}}$[12] and a plasmon-exchange contribution.

IV. NUMERICAL RESULTS IN THE HIGH-DENSITY LIMIT

The continuum contribution in (18) can be interpreted as arising from electrons annihilating with varying momentum p within the Fermi sea. The case of zero-electron momentum was considered and the q integration in (18) was performed on the electronic digital computer SMIL at the University of Lund, Lund, Sweden. Since rough calculations indicated a slow variation of the integrand in (18) with p we will, at this stage, simply ignore this dependence.

It is convenient to quote the resulting densities $n^{(1)}$ continuum in units of the free-Sommerfeld density n_0 for the material. The values obtained for electron gas densities encompassing the metals Na and Al are listed in Table I. Also listed are similar densities calculated in perturbation theory from the screened potential of K(I). Apparently the Bohm-Pines model predicts overly large annihilation rates. It then seems justified to redo the calculation of K(I) using the screened potential obtained in the high-density limit.

We have also estimated the plasmon contribution to the density enhancement. This has been done by assuming the coupling of the electron-positron pair through plasmons is independent of momentum, i.e.,

$$R_q\approx R_0=\Omega_0/4 \quad \text{and also} \quad \Omega_q\approx\Omega_0,$$

where Ω_0 is the classical plasmon frequency. The numerical results are displayed in Table II. The influence of the plasmon on annihilation rates will clearly be small.

Taking together the continuum and plasmon contributions we have listed in Table II the annihilation rates

TABLE I. Density corrections $n^{(1)}{}_{\text{continuum}}$ in units of n_0 due to the short-range forces $u^{\text{h.d.}}$, $u^{\text{K(I)}}$, u^s in first order.

r_s[a]	High-density limit	K(I) (first order)	Static limit (first order)
2	1.080	1.329	1.066
3	1.492	1.993	1.496
4	1.862	2.658	1.891

[a] r_s is the familiar density parameter giving the radius of a sphere, in units of the Bohr radius, containing on the average one electron.

[12] It is easily demonstrated that $v_q{}^{\text{h.d.}}$ is of short range since $v_q{}^{\text{h.d.}}$ is convergent in the limit $q\to 0$.

TABLE II. Plasmon contribution to the electron density, in units of n_0, near the positron and comparison between the mean lifetimes to be expected in the high-density limit and that due to Bell and Jørgensen.

r_s	Plasmon contribution to density	Annihilation rates in high-density limit (10^{-9} sec^{-1})	Experimental annihilation rates (10^{-9} sec^{-1})
2	0.158	3.319	5.35
3	0.289	1.199	3.82
4	0.354	0.594	3.33

to be expected in the high-density limit. These rates can be compared with those due to Bell and Jørgensen.[3] Although Al is not badly represented by the high-density limit, metals with less dense electron gases are far from adequately described.

V. EXTENSION TO LOWER DENSITIES

We will now lift the restrictions of the previous paragraphs and attempt to solve Eq. (2) to all orders in the effective interaction $u(x)$. It is immediately plausible and readily demonstrable[13] that Eq. (2) could be reduced to a Schrödinger-like equation if the potential $u(x)$ were static. In this case it is possible to obtain

$$n=(1/V)\sum_{p<k_F}|\Psi_p(\mathbf{x},\mathbf{x})|^2, \quad (19a)$$

where $\Psi_p(\mathbf{x},\mathbf{x})$ can be interpreted as the wave function for a positron together with an electron of momentum p within the Fermi sea. If we introduce the Fourier representation

$$\Psi_p(\mathbf{x}_e,\mathbf{x}_p)=\sum_{rs} e^{i(\mathbf{x}_e\cdot\mathbf{r}+\mathbf{x}_p\cdot\mathbf{s})}\Psi_p(\mathbf{r},\mathbf{s}), \quad (19b)$$

then the momentum wave function satisfies

$$\Psi_p(\mathbf{r},\mathbf{s})=\delta_{\mathbf{r}\mathbf{p}}\delta_{\mathbf{s}0}$$
$$-\frac{Q_{rs}{}^+}{(r^2+s^2)-p^2}\frac{1}{V}\sum_{\rho\sigma} u_{\mathbf{r}\mathbf{s}\rho\sigma}{}^{\text{static}}\Psi_p(\boldsymbol{\rho},\boldsymbol{\sigma}), \quad (20)$$

where $Q_{rs}{}^+=0$ if either $r<k_F$ or $s=0$, i.e., $Q_{rs}{}^+$ accounts for the exclusion principle in intermediate states. Equations (19a) and (20) are equivalent to (2) and (3) when the electron and positron interact through an instantaneous interaction.

If we wish to make use of Eq. (20) we must somehow obtain a static equivalent to $u(x)$. To check the effect of the frequency dependence of $u_k(\omega)$ we chose the simplest equivalent

$$u_k{}^s=u_k(0), \quad (21)$$

and recalculated the continuum density correction $n^{(1)}$ for a zero-momentum electron. The results are contained

[13] We will not include a proof of this statement here as it is rather tedious. In any case the establishment of Eqs. (19a) and (20) resembles closely the development of the Bethe-Goldstone equation. See for example, A Klein and R. E. Prange, Phys. Rev. 112, 1008 (1958).

in Table I from which it is evident that the first-order density corrections arising from $u_k(\omega)$ and $u_k(0)$ are indistinguishable. It is reasonable then to use (21) as specifying our choice of a static potential.

By eliminating the frequency dependence of $u_k(\omega)$ we are, of course, not ignoring the recoil of either the positron or the electron with which it is interacting. It would appear, however, that our results are insensitive to the inertia of the background gas producing the screening. The equivalence of $u_k(0)$ and $u_k(\omega)$ cannot be expected to be as exact for the interaction of the positron with an electron at the surface of the Fermi sea. Nevertheless we have used the same static potential throughout the Fermi sea.

VI. NUMERICAL SOLUTION OF THE ELECTRON-POSITRON SCHRÖDINGER EQUATION

In the limit of infinite volume (20) becomes

$$\Psi_p(\mathbf{r})=\delta(\mathbf{r}-\mathbf{p})-\frac{Q_r}{\mathbf{r}^2+(\mathbf{p}-\mathbf{r})^2-\mathbf{p}^2}\frac{1}{(2\pi)^3}\times\int d^3\rho\, u^s(\mathbf{r}-\boldsymbol{\rho})\Psi_p(\rho). \quad (22)$$

In obtaining (22) we have explicitly taken into account momentum conservation and suppressed the positron momentum label. It is convenient to concentrate on the departure of the wave function Ψ_p from a plane wave. We write

$$\Psi_p(\mathbf{r})=\delta(\mathbf{r}-\mathbf{p})+Q_r+X_p(\mathbf{r}) \quad (23)$$

and obtain

$$X_p(\mathbf{r})=-u^s(\mathbf{r}-\mathbf{k})\frac{1}{\mathbf{r}^2+(\mathbf{p}-\mathbf{r})^2-\mathbf{p}^2}-\frac{1}{\mathbf{r}^2+(\mathbf{p}-\mathbf{r})^2-\mathbf{p}^2}\frac{1}{(2\pi)^3}\times\int_{\rho>k_F} d^3\rho\, u^s(\mathbf{r}-\boldsymbol{\rho})\chi_p(\boldsymbol{\rho}). \quad (24)$$

The latter equation must, in general, be solved for electron momenta $p<k_F$. The exclusion principle tends to smooth out the dependence of annihilation rate on electron momentum, inhibiting the interaction of the positron with electrons deep within the Fermi sea and enhancing that with electrons at the surface. We have then tried to treat accurately the case $p=0$ and estimate the finite momentum corrections as a perturbation.

For an electron at the center of the sea (24) becomes

$$\chi_0(\mathbf{r})=-\frac{u(\mathbf{r})}{2\mathbf{r}^2}-\frac{1}{(2\pi)^3}\frac{1}{2\mathbf{r}^2}\int_{\rho>k_F} d^3\rho\, u^s(\mathbf{r}-\mathbf{p})\chi_0(\boldsymbol{\rho}). \quad (25)$$

A spherically symmetric solution of (25) may be obtained by assuming $\chi_0(\boldsymbol{\rho})$ is independent of the angles of $\boldsymbol{\rho}$. The reduced integral equation reads

$$\chi_0(r)=-\frac{u(r)}{2r^2}-\frac{1}{2r^2}\frac{4\pi}{(2\pi)^3}\int\rho^2 d\rho\, u_0(r,\rho)\chi_0(\rho) \quad (26)$$

with

$$u_0(r,\rho)=\frac{1}{4\pi}\int d\Omega_\rho\, u(\mathbf{r}-\mathbf{p}).$$

A discussion of the numerical solution of (26), performed on SMIL, is contained in the Appendix.

An electron of finite momentum presents some difficulties since (25) cannot then be separated into partial waves. There is still axial symmetry in the problem and one can write

$$\chi_p(\mathbf{r})=\sum_{l=0}^{\infty} P_l(\cos\theta)\chi_p{}^l(r), \quad (27)$$

where θ is the angle between $\mathbf{p}$ and $\mathbf{r}$.

In addition, reflection symmetry in the plane $\theta=\pi/2$ implies that insertion of (27) into (25) will not result in a coupling of even with odd l. We have made the simplest approximation

$$\chi_p(\mathbf{r})\approx\chi_p{}^0(r). \quad (28)$$

An angular averaging of (25) then leads to

$$\chi_p{}^0(r)=\frac{1}{4\pi}\int d\Omega_p\left(\frac{-u(\mathbf{r}-\mathbf{p})}{\mathbf{r}^2+(\mathbf{p}-\mathbf{r})^2-\mathbf{p}^2}\right)-\frac{1}{4\pi}\int d\Omega^p\frac{1}{\mathbf{r}^2+(\mathbf{p}-\mathbf{r})^2-\mathbf{p}^2}\times\frac{1}{(2\pi)^3}\int\rho^2 d\rho\, u_0(r,\rho)\chi_\rho{}^0(\rho). \quad (29)$$

The latter equation is very similar in form to (26) and the numerical treatment is identical. Because of the assumed smooth variation of annihilation rate with electron momentum we have treated (29) only for $p=\frac{1}{2}k_F, \frac{3}{4}k_F$.

The calculations discussed were performed for three values of the electron density specified by $r_s=2, 3, 4$. The extreme ends of this density range correspond roughly to Al and Na. We have quoted for each electron density and momentum an enhancement factor:

$$\epsilon(\gamma)=|\psi_p(\mathbf{x},\mathbf{x})|^2+\epsilon_{\text{plasmon}},\quad \gamma=p/k_F, \quad (30)$$

which is a measure of the increased electron density at

TABLE III. Momentum dependence of enhancement factors $\epsilon(\gamma)$ for varying electron gas densities.

r_s	$\gamma=0$	$\gamma=\frac{1}{2}$	$\gamma=\frac{3}{4}$
2	3.480	3.655	3.941
3	6.172	6.555	7.204
4	11.225	12.124	13.708

TABLE IV. Annihilation rate for positrons in metals of different densities obtained by use of the momentum-dependent enhancement $\epsilon(\gamma)=a+b\gamma^2+c\gamma^4$.

r_s	a	b	c	Annihilation rate (10^{-9} sec^{-1})
2	3.480	0.600	0.387	5.930
3	6.172	1.292	0.967	3.239
4	11.225	2.940	2.617	2.609

the positron. These enhancement factors are listed in Table III.

A final annihilation rate was obtained by performing an averaging over the Fermi sea assuming a momentum dependence of the form

$$\epsilon(\gamma)=a+b\gamma^2+c\gamma^4. \tag{31}$$

The constants a, b, c and the annihilation rate determined for each electron gas density are listed in Table IV. We may also use the information in this latter table to obtain the angular correlation to be expected between the two quanta emitted in the annihilation of an electron-positron pair.

Assuming the positron is at rest we can calculate the number of γ-ray pairs possessing a total momentum p_z, in some fixed direction, by integrating (31) over an appropriate plane intersection of the Fermi sea. We obtain the distribution function

$$P(\gamma_z)=\text{constant}\int_{\gamma_z}^{1}\gamma d\gamma\,\epsilon(\gamma) \tag{32}$$

provided we assume an isotropic density for the electrons in the sea. If $\epsilon(\gamma)$ is roughly constant over the sea (32) will give the familiar inverted parabola distribution observed for many metals.[14]

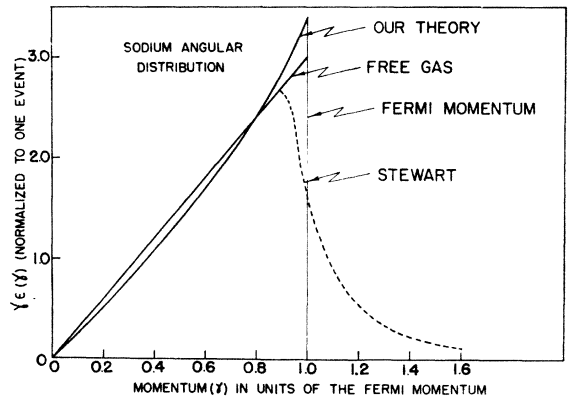

FIG. 3. Variation of the enhancement factor $\gamma\epsilon(\gamma)$ across the Fermi sea, for $\gamma=p/k_F=0$ to $\gamma=1$. Our theory is compared to the free electron gas. The form of Stewart's experimental results near the Fermi surface is indicated.

As an example we have considered the case of Na which has been treated experimentally most recently by Stewart,[15] who is able to differentiate his data numerically and obtains a plot of $\gamma\epsilon(\gamma)$. In Fig. 3 we have plotted this quantity for a free gas and for our theory. It is difficult to say just what is the best curve through Stewart's points. One may say though that his general results are not inconsistent with ours except perhaps near $\gamma=1$, the surface of the Fermi sea.

Stewart's work certainly contains events corresponding to a total momentum for the annihilating pair greater than the Fermi momentum. The possibility of annihilation involving electrons of momenta $p>k_F$ was artificially eliminated in our work. Such momentum states could be populated by interaction of electrons with the lattice or by electron-electron interactions within the gas. High-momentum components may be present in the positron wave function due to its departure from a plane wave near the ion centers (excluded volume effect).[16] Finally annihilation with core electrons would add broad tails to the free gas distribution (32). The experimental picture for trivalent Al is even more interesting in that it shows greater departure from the free gas near the Fermi surface.

VII. DISCUSSION AND CONCLUSIONS

A surprisingly accurate description of the total annihilation rate in many metals can be obtained by iterating the screened electron-positron potential deduced in the high-density limit. This can be seen in Fig. 4 where the experimental annihilation rates due to Bell and Jørgensen[2] are compared with those obtained from our theory. Both the absolute rate and the variation with electron density are adequately described.

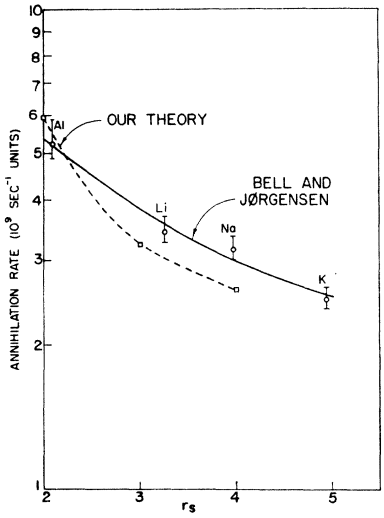

FIG. 4. Variation of annihilation rate with valence electron density. Our theory is compared to the experimental work of Bell and Jørgensen.

[14] G. Lang, S. DeBenedetti, and R. Smoluchowski, Phys. Rev. **99**, 596 (1955). A. T. Stewart, Can. J. Phys. **35**, 168 (1957); Phys. Rev. **123**, 1587 (1961).

[15] A. T. Stewart, Phys. Rev. **123**, 1587 (1961).

[16] S. DeBenedetti, C. E. Cowan, W. R. Konneker, and H. Primakoff, Phys. Rev. **77**, 205 (1950).

It is perhaps most surprising that the less dense metals are so well accounted for. This result can be made more plausible by examining the extreme low density limit. One would expect the positron to become more or less correlated with a single electron in a quasi-positronium atom. There would still be, however, sufficient exchange and interaction for the complete mixing of triplet and singlet spin states. The lifetime in the low-density limit should then be $\sim 4\times(1.25\times 10^{-10}$ sec$)=5\times 10^{-10}$ sec. But we have included just those interactions which would lead eventually to the bound state. Hence our calculations have a good chance of predicting the lifetimes of the lower density gases.

One might say that the positron is a poor probe of the electron gas because it appreciably distorts the initial metal configuration. One can perhaps assume our calculations describe this distortion adequately and now try to include more details of a real metal. It would seem most hopeful to concentrate on the region near the surface of the momentum distribution where effects of the lattice and electron-electron interactions should be most noticeable. Very recently, Stewart[17] has measured the angular distribution of annihilation quanta for Be along three distinct crystal directions. He has found three distinct distributions, thus vividly demonstrating the anisotropy of the electron momentum distribution.

Finally we would like to point out the existence of a long lifetime in the metallic decay schemes. Bell and Jørgensen[3] have observed in the alkalis a weak decay mode of lifetime approximately twice that of the main component. It is difficult to see how such a mode could arise from annihilation in the electron gas. If real, this long-lived component may arise from an electron-positron state spatially localized in the sample surface or perhaps near a metallic ion. We have made no attempt to account for this state.

ACKNOWLEDGMENTS

The hospitality of the late Professor Niels Bohr and Professor Aage Bohr at the Institute for Theoretical Physics in Copenhagen is greatly appreciated. The author would like to thank Professor Aage Bohr for helpful suggestions and encouragement during the preparation of this work. In addition, he would like to thank Dr. G. E. Lee-Whiting of Atomic Energy of Canada Limited, Chalk River and Professor P. R. Wallace, McGill University, for many clarifying conversations.

The numerical work in this paper would have been impossible without the excellent assistance of L. Silverberg, K. Jonsson and Laborator Froberg of the University of Lund. The author is very appreciative of this aid. The help of the secretarial staff of A.E.C.L., Chalk River in the preparation of the manuscript is gratefully acknowledged.

[17] A. T. Stewart (private communication).

APPENDIX

We are attempting to solve the equation

$$\chi_0(r)=-\frac{1}{(2\pi)^3}\frac{u(r)}{2r^2}-\frac{1}{2r^2}\frac{4\pi}{(2\pi)^3}\int_{k_F}\rho^2 d\rho\, u_0^s(r,\rho)\chi_0(\rho) \quad \text{(A1)}$$

with

$$u_0^s(r,\rho)=\frac{1}{4\pi}\int d\Omega_\rho\, u^s(|\mathbf{r}-\boldsymbol{\rho}|). \quad \text{(A2)}$$

It is convenient from the outset to state momenta in units of k_F. This may be achieved by multiplying (A1) throughout by k_F^3. A convenient parameter to use in this analysis in place of r_s is

$$\tau=2/\pi a_0 k_F\approx 0.33 r_s. \quad \text{(A3)}$$

In these units the static interaction is

$$u^s(k)=-\frac{\tau(2\pi^2)}{k^2}\times\frac{1}{\{1+(\tau/k^3)[k+(1-\frac{1}{4}k)\ln|(k+2)/(k-2)|]\}}. \quad \text{(A4)}$$

The angular average in (A2) then appears as

$$u_0(r,\rho)=+\frac{1}{2}\int_{|r-\rho|}^{|r+\rho|} dk\, k u(k). \quad \text{(A5)}$$

The general procedure followed was to select a grid of points $\{r_0\}$ along the r axis in (A1) and to evaluate (A5) for r, ρ assuming values in this grid. Then a numerical integration formula (in this case three point Gaussian integration) was used to convert (A1) into a set of linear equations in the unknowns $\chi_0(r_i)$. The latter equations were subsequently solved by Crout elimination.

The grid selected consisted of thirty points extending from $r=1$ to $r=40$. The grid was taken finer for smaller r to capitalize on the expected asymptotic behavior of the solution, i.e.,

$$\chi_0(r)\xrightarrow[r\to\infty]{} 1/r^4. \quad \text{(A6)}$$

The greatest difficulties were encountered in the computation of the kernel $u_0(r,\rho)$. The potential (A4) clearly has a singularity in slope at $k=2$, a singularity of no particular physical significance. We used expansions of $u^s(k)$ in powers of $(k/2)$ or $(2/k)$ valid for $k<2$ and $k>2$, respectively. The region immediately near $k=2$ was ignored, note being taken of a cancellation occurring in this region. The integral $\int_1^{40} r^2 dr\, \chi_0(r)$ was calculated from the solution obtained. The integral from $r=40$ to $r=\infty$ was estimated from the asymptotic behavior (A6) which was demonstrated in the course of calculation.

For initial electron momenta differing from zero the numerical procedure was essentially identical.